S4 Movement in a Mammalian HCN Channel

Sriharsha Vemana, Shilpi Pandey, and H. Peter Larsson

Neurological Sciences Institute, Oregon Health and Science University, Beaverton, OR 97006

ABSTRACT Hyperpolarization-activated, cyclic nucleotide–gated ion channels (HCN) mediate an inward cation current that contributes to spontaneous rhythmic firing activity in the heart and the brain. HCN channels share sequence homology with depolarization-activated Kv channels, including six transmembrane domains and a positively charged S4 segment. S4 has been shown to function as the voltage sensor and to undergo a voltage-dependent movement in the Shaker K^+ channel (a Kv channel) and in the spHCN channel (an HCN channel from sea urchin). However, it is still unknown whether S4 undergoes a similar movement in mammalian HCN channels. In this study, we used cysteine accessibility to determine whether there is voltage-dependent S4 movement in a mammalian HCN1 channel. Six cysteine mutations (R247C, T249C, I251C, S253C, L254C, and S261C) were used to assess S4 movement of the heterologously expressed HCN1 channel in *Xenopus* oocytes. We found a state-dependent accessibility for four S4 residues: T249C and S253C from the extracellular solution, and L254C and S261C from the internal solution. We conclude that S4 moves in a voltage-dependent manner in HCN1 channels, similar to its movement in the spHCN channel. This S4 movement suggests that the role of S4 as a voltage sensor is conserved in HCN channels. In addition, to determine the reason for the different cAMP modulation and the different voltage range of activation in spHCN channels compared with HCN1 channels, we constructed a COOH-terminal–deleted spHCN. This channel appeared to be similar to a COOH-terminal–deleted HCN1 channel, suggesting that the main functional differences between spHCN and HCN1 channels are due to differences in their COOH termini or in the interaction between the COOH terminus and the rest of the channel protein in spHCN channels compared with HCN1 channels.

KEY WORDS: voltage sensor • hyperpolarization activated • cysteine accessibility • SPIH

INTRODUCTION

Hyperpolarization-activated, cyclic nucleotide–gated ion channels (HCN) channels are members of the super family of voltage-gated ion channels and are activated by membrane hyperpolarization (Santoro and Tibbs, 1999; Robinson and Siegelbaum, 2003). The opening of the channel generates an inward current that raises the membrane potential of a cell toward threshold. This inward current enables HCN channels to regulate rhythmic activity in cells such as "pacemaker" cells in the heart or neurons in the thalamus (Santoro and Tibbs, 1999; Robinson and Siegelbaum, 2003). HCN channels share the greatest sequence homology with depolarization-activated Kv channels (Santoro and Tibbs, 1999). Both HCN and Kv channels are tetramers, with each subunit containing six transmembrane segments, a positively charged S4 segment, a pore loop between S5 and S6, and a GYG sequence motif in the selectivity filter (see Fig. 2 A). However, HCN channels, unlike Kv channels, possess a cyclic nucleotide binding domain at the COOH terminus, which allows intracellular, second-messenger molecules, like cAMP or cGMP, to modulate the activity of HCN channels (Robinson and Siegelbaum, 2003).

The S4 domain in voltage-gated ion channels contains positive charges spaced at every third residue and is the most conserved domain among voltage-gated ion channels. S4 was hypothesized early on to be the voltage sensor in voltage-gated ion channels. S4 is relatively conserved between the depolarization-activated Kv channels and the hyperpolarization-activated HCN channels (Fig. 2 A). Shaker K^+ channels have seven basic residues in the S4 domain. Mammalian HCN channels have nine basic residues, spaced at every third residue within S4. A neutral serine residue divides these nine residues into two groups, one of four and one of five (Fig. 2 A). The spHCN channels have eight basic residues that a neutral serine divides into two groups of four. Despite similarities between HCN and Kv channels, HCN channels open by hyperpolarizing potentials and close by depolarizing potentials, in contrast to Kv channels, which open during depolarizations and close by hyperpolarizations.

The difference in voltage dependence between HCN and Kv channels is even more intriguing in the context

Address correspondence to H. Peter Larsson, Neurological Sciences Institute, Oregon Health & Science University, 505 NW 185th Ave., Beaverton, OR 97006. Fax: (503) 418-2501; email: larssonp@ohsu.edu

Abbreviations used in this paper: HCN, hyperpolarization-activated, cyclic nucleotide–gated ion channels; MTSEA, methanethiosulfonate-ethylammonium; MTSET, methanethiosulfonate ethyltrimethylammonium; TNB, 5-thio-2-nitrobenzoate.

J. Gen. Physiol. © The Rockefeller University Press • 0022-1295/2004/01/21/12 $8.00
Volume 123 January 2004 21–32
http://www.jgp.org/cgi/doi/10.1085/jgp.200308916

of recent findings showing that S4 in the sea urchin sperm clone (spHCN) and S4 in a bacterial HCN channel (MVP) move in a manner similar to the movement of S4 in depolarization-activated Kv channels (Shaker) (Männikkö et al., 2002; Sesti et al., 2003). Previous studies have shown S4 to be the voltage sensor in Shaker K^+ channels (Aggarwal and MacKinnon, 1996; Larsson et al., 1996; Seoh et al., 1996; Yusaf et al., 1996; Baker et al., 1998), where S4 moves outward during depolarization and channel opening, and inward during hyperpolarization and channel closing (Larsson et al., 1996; Baker et al., 1998). S4 in spHCN channels has a similar movement, except that in these channels, inward movement opens the channels and outward movement closes them (Männikkö et al., 2002).

spHCN channels are one of several types of cloned HCN channels, including several cloned from mammalian sources (mouse, human, rat, and rabbit) (Gauss et al., 1998; Ludwig et al., 1998; Santoro et al., 1998). There are many functional differences among the HCN channel clones, but especially significant are those differences between mammalian HCN (HCN1–4) channels and spHCN channels. Mammalian HCN channels activate at more hyperpolarized potentials than spHCN channels (Gauss et al., 1998; Ludwig et al., 1998). In addition, cAMP shifts the voltage dependence of activation in mammalian HCN channels to more depolarized potentials, while cAMP increases the amplitude of currents through spHCN channels and removes a time-dependent inactivation that is present at low cAMP concentrations (Gauss et al., 1998; Ludwig et al., 1998).

Previous investigations into the role of the S4 domain in mammalian HCN channels involved mutating basic residues in the S4 of the HCN2 channel to neutral amino acids (Chen et al., 2000; Vaca et al., 2000). The neutralization of basic residues in S4 resulted in a shift of the voltage-dependent activation to more hyperpolarizing potentials. These findings are significant in highlighting the importance of S4 in mammalian HCN channels. However, S4 movement in mammalian HCN channels has not been shown. The focus of our study was to utilize cysteine accessibility methods (Männikkö et al., 2002) to measure whether S4 in mammalian HCN1 channels moves during changes in membrane potential and whether S4 functions similarly to the voltage sensor in spHCN channels.

MATERIALS AND METHODS

The experiments were performed on the mouse HCN1 channel and the sea urchin spHCN channel expressed in *Xenopus* oocytes. It has been shown that the endogenous cysteine C318 in HCN1 channels is extracellularly accessible to MTS reagents (Xue and Li, 2002). In our experiments, C318 was mutated to a serine, producing HCN1 channels with currents that were not modified by the extracellular application of methanethiosulfonate ethyltrimethylammonium (MTSET). The C318S mutation was subsequently used as a background HCN1 channel in which all cysteine mutations were made. In addition, to remove six of the intracellularly located cysteines and to eliminate the potential influence of cyclic nucleotides on the voltage dependence of HCN1 channels, the channels used in this study had the cyclic nucleotide binding site domain removed by introducing a stop codon at residue S391 (Wainger et al., 2001). Similarly, we created a COOH-terminal–deleted spHCN channel, $spHCN_{\Delta C\text{-term}}$, by introducing a stop codon at the corresponding site S472 in the spHCN channel.

Molecular Biology

Site-directed mutagenesis was performed on C318S HCN1 channels using the QuikChange Kit (Stratagene). Initially, only charged residues were mutated to cysteines because it is the movement of charged residues that is most important in studying a voltage-gated ion channel. Lack of expression (see Fig. 2 A) of several of these charged residues led us to mutate adjacent, noncharged residues in order to test for voltage dependent S4 movement (Fig. 2 A). Residue K256 was excluded from our study due to the lack of expression that K256 mutants have exhibited in earlier studies (Chen et al., 2000; Vaca et al., 2000; Männikkö et al., 2002). The plasmid was linearized with NheI. RNA was synthesized in vitro using the T7 mMessage mMachine kit (Ambion) and injected (50 nl of 0.1–1 ng/nl) into *Xenopus* oocytes. The electrophysiology experiments were performed 2–6 d after the injection of mRNA. The lack of expression for a mutant was defined as no currents in a two-electrode voltage clamp from at least three different RNA injections and at least two different clones.

Electrophysiology

Cysteine-substituted mutant channels expressed in *Xenopus* oocytes were recorded with the two-electrode voltage clamp technique for extracellular accessibility studies and the patch-clamp technique for the intracellular accessibility studies. Microelectrodes were made from borosilicate glass and filled with a 3M KCl solution for the two-electrode experiments. Each electrode had a resistance of 0.5–1.0 MΩ. All experiments were performed at room temperature.

Two-electrode Voltage-clamp Technique

Whole-cell ion currents were measured with the two-electrode voltage-clamp technique, using a CA-1B amplifier (Dagan Corp.). The bath solution consisted of a 100-K solution (in mM): 89 KCl, 15 HEPES, 0.4 $CaCl_2$, and 0.8 $MgCl_2$. KOH was added to adjust the pH to 7.4, yielding a final K^+ concentration of 100 mM. The use of the 100-K solution produced larger amplitude currents, which allowed for better monitoring of current changes at the negative voltage pulse. During the recording of R247C, the bath solution consisted of a 1-K solution of (in mM): 1 KCl, 88 NaCl, 15 Hepes, 0.4 $CaCl_2$, and 0.8 $MgCl_2$. The pH was adjusted to 7.4 by the addition of NaOH. The use of the 1-K solution allowed for monitoring of changes in the tail currents at 0 mV, a potential that reduced the effects of contaminating leak currents.

Patch Voltage-clamp Technique

The macro-patch currents were measured with the patch-clamp technique (Axopatch 200B; Axon Instruments, Inc.). The extracellular pipette solution consisted of a 100-K solution (described above) and 1 mM $BaCl_2$ to block endogenous, single K^+-channel events. The intracellular patch solution consisted of (in mM): 98

KCl, 0.5 $MgCl_2$, 0.1 $CaCl_2$, 1 EGTA, 10 HEPES, and 1 ATP. KOH was used to adjust the pH to 7.1.

Cysteine Labeling and Accessibility Studies

Cysteine residues were substituted, one at a time, for seven residues in the HCN1 S4 domain (see Fig. 2 A). Cysteine residues react with MTS reagents much faster ($>10^6$) in an aqueous environment than in an hydrophobic environment (Karlin and Akabas, 1998); thus, the modification rate of a cysteine by a MTS reagent depends on whether the cysteine is located in the extra- or intracellular solution, or is buried in the membrane. Changes in the accessibility of cysteine residues were tested by measuring the voltage dependence of the rate of irreversible covalent modification with the cysteine-specific compounds MTSET and methanethiosulfonate-ethylammonium (MTSEA). The MTS reagents (100 μM to 2 mM) were dissolved in a 100-K solution and kept on ice until they were applied to the bath. A new MTS solution was made every 4 h. A gravity-driven perfusion system was used in the application and the wash-out of MTS reagents. The time constant for the solution exchange was ~1 s (tested by applying 0.2 mM $CsCl_2$, which blocks ~50% of the HCN1 channels). The fast solution exchange ensured that the 10-s application and 20-s wash-out times were adequate enough to expose the oocyte to MTSET only at the desired potential. The MTS modification of the cysteine was monitored by a change in the current amplitude of the channel at a specific test voltage. This test voltage was chosen from a comparison of current/voltage plots before and after application of MTS reagents (see next section). Cysteine mutations that did not display any change in the current during the MTS treatment were not used to draw conclusions about cysteine accessibility.

A two-electrode voltage clamp was used to test for the extracellular accessibility of cysteines to MTSET. The patch-clamp technique was used to test for intracellular accessibility of cysteines to MTSEA that was applied to the cytosolic face of inside-out patches. A comparison of current/voltage curves before and after MTS application allowed us to determine the ideal test voltage for each residue, that is, the voltage at which the difference in current amplitude is maximal between pre and post-MTS application.

The extracellular modification protocol started at a holding potential of 0 mV, followed by a 200-ms step to the ideal test voltage determined for the residue (for example −120 mV for S253C). This voltage step was followed by a step to +50 mV, and in turn by a 30-s step to either 0 mV or −100 mV. The application of MTSET occurred during the first 10 s of the 30-s step. The extracellular solution was perfused for the last 20 s to wash away any unbound MTSET.

The intracellular accessibility of the introduced cysteines was tested using MTSEA because the application of MTSET consistently destroyed the excised patches clamped to the very hyperpolarized voltage steps (−120/−140 mV) that were needed to open the HCN1 channels. A similar effect has been reported for patch clamp experiments using very negative potentials and MTSET on excised patches containing Shaker K channels (Baker et al., 1998; Yang and Sigworth, personal communication). However, this effect was not seen with MTSEA. In addition, run-down was significant upon excising the patch (Chen et al., 2001). The run-down was seen in all excised patch experiments; 5 min after patch excision, the current in response to a voltage step to −130 mV was reduced by 57% ± 7.5%. Therefore, to minimize the effect of run-down, we excised the patches directly into a bath solution containing 100 μM MTSEA for L254C and 200 μM MTSEA for S261C. We tested the state dependence of internal cysteine accessibility by applying different voltage protocols while the cytosolic face of the patch was exposed to the MTSEA bath solution. The closed state accessibility was tested using a 200-ms test pulse every 10 s from a holding potential of 0 mV (>90% of the time spent at 0 mV). Open state accessibility was tested using a 1-s hyperpolarizing voltage pulse every 2 s from a holding potential of 0 mV (50% of the time spent at hyperpolarized potentials). In some experiments, 20 mM cysteine was included in the pipette solution to scavenge MTSEA that diffused across the patch membrane (Holmgren et al., 1996; Karlin and Akabas, 1998). The addition of the 20 mM cysteine in the pipette solution did not alter the modification rates, indicating that the MTSEA modification was intracellular.

These protocols allowed us to measure the time course of modification with changes in the amplitude of the current plotted against exposure time (time [s] × concentration MTSET [mM]). From these plots, a monoexponential curve was fitted and a pseudo first-order modification rate constant, k, was calculated from the time constant, $k = 1/\tau$ [$mM^{-1}\ s^{-1}$]. The potential used to test for open-state accessibility was more negative for internal accessibility than for external accessibility because the G(V) shifts to more negative potentials after patch excision.

MTS Reagent Stability

An important consideration in using MTS reagents is their stability during the cysteine accessibility experiments. Ideally, solutions should be made immediately before their use in experiments. However, MTS reagents in solutions maintained on ice have been shown to be relatively stable for several hours (Stauffer and Karlin, 1994). We repeated an assay developed by Stauffer and Karlin (1994) to determine the half-times for hydrolysis of MTS reagents both in the solution used for this paper, i.e., 100-K solution (see above), as well as the solution used by Stauffer and Karlin (1994), i.e., NP100; (100 mM NaCl, 10 mM $NaPO_4$, 1 mM EDTA, 3 mM NaN_3, pH 7.0). The assay tests for the formation of a mixed disulfide bond between the methanethiosulfonate-reactive group and 5-thio-2-nitrobenzoate (TNB). 100 μM TNB was formed from the reaction of 50 μM DTT with 2 mM DTNB (5,5′-dithiobis(2-nitrobenzoate)) (Stauffer and Karlin, 1994). TNB has a maximum absorbance at 412 nm (Stauffer and Karlin, 1994). The reaction of TNB with a MTS reagent causes a decrease in absorbance, thus allowing a quantitative measure of the nonhydrolyzed MTSET concentration in a solution. Initially, we measured the absorbance at 412 nm of 100 μM TNB with varying concentrations of MTSET dissolved in the 100-K solution in a quartz cuvette to generate a standard linear curve (Fig. 1 A). Next, the stability of MTSET on ice or at room temperature was tested. MTSET was dissolved in a 100-K solution, in a NP100 solution, or in dH_2O that was kept on ice or at room temperature. At various time points from 0 to 500 min, 100 μl of MTSET was taken from the 100-K solution or the NP100 solution, and was added to the TNB solution for a final MTSET concentration of 50 μM. 50 μM was used because it was in the middle of the linear plot shown in Fig.1 A. The absorbance of the MTSET/TNB solutions from the various time points were used, together with the standard curve (Fig. 1 A), to calculate the remaining nonhydrolyzed MTSET concentration after incubation on ice or at room temperature (Fig. 1 B). The results from this assay show that MTSET (even at physiological pH) maintained on ice was stable for at least 4 h, the maximum duration of our experiments. It is interesting that MTSET in our 100-K solution at room temperature had a half-life of 2 h, whereas MTSET in NP100 at room temperature had a much faster decay rate ($t_{1/2}$ = 13 min). This faster rate of hydrolysis in NP100 is partly due to the presence of sodium azide in the NP100 solution, which accelerated the decay of MTSET (unpublished data).

The results from this assay show that MTSET hydrolysis was not a detrimental factor during the experiments reported here.

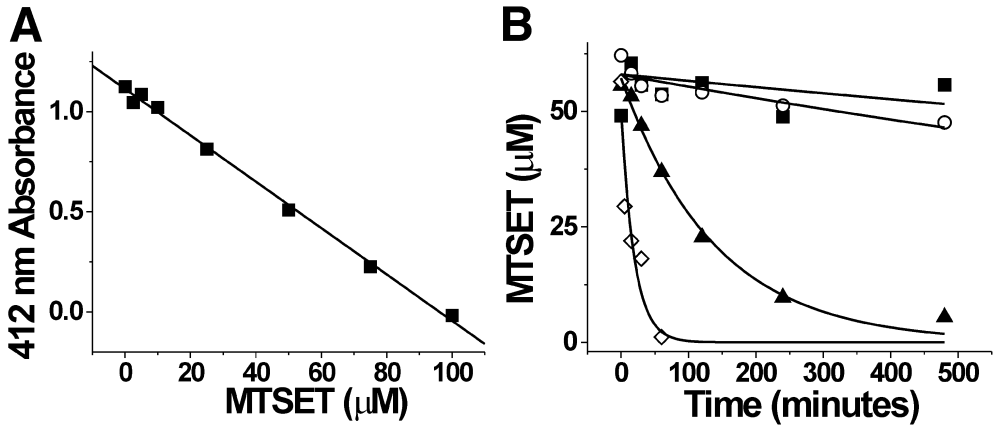

FIGURE 1. Stability of MTSET at room temperature and on ice. (A) Absorbance at 412 nm of 100 μM TNB dissolved in the 100-K solution containing different concentrations (0–100 μM) of MTSET. (B) A plot comparing the stability of MTSET over time in different solutions and at different temperatures. (■) MTSET in 100-K solution on ice, τ = 1420 ± 312 min; (○) MTSET in dH_2O on ice, τ = 4113 ± 3000 min; (▲) MTSET in 100-K solution at room temperature, τ = 111 ± 8 min; and (◇) MTSET in NP100 solution at room temperature, τ = 19.4 ± 6.6 min.

RESULTS

To test for S4 movement in HCN1 channels, we introduced cysteines at 11 residues in the S4 domain, one at a time (Fig. 2 A), in order to determine the accessibility of the cysteine mutants to the MTS reagents applied in the extracellular and intracellular solutions. Of the 11 mutations, K250C, L252C, L258C, R259C, and L260C did not express. Fig. 2 B shows HCN1 currents from the HCN1 C318S mutant used as the background (see MATERIALS AND METHODS), and Fig. 2 C shows the conductance-versus-voltage curve, G(V), for the expressing mutations.

The S4 domain is relatively well conserved among HCN1, spHCN, and Shaker K^+ channels (Fig. 2 A). Earlier studies have shown that cysteines introduced at positions 338 in spHCN channels and 368 in Shaker K^+ channels were accessible to MTSET from the intracellular solution at hyperpolarized potentials and from the extracellular solution at depolarized potentials, suggesting a complete transmembrane movement of these residues (Larsson et al., 1996; Baker et al., 1998; Männikkö et al., 2002). Therefore, we initially focused on the corresponding residue 253 in HCN1 channels to determine whether this residue has a similar, voltage-dependent transmembrane movement.

We found that the extracellular application of MTSET dramatically increased the activation rate for S253C (Fig. 3, A–C). Extracellular MTSET modified

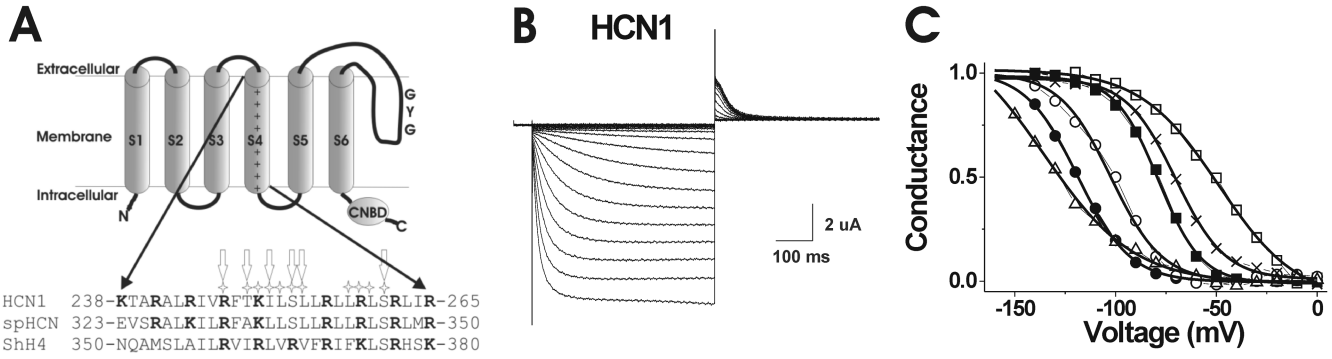

FIGURE 2. Membrane topology and sequence alignment of HCN1 channels. (A) Above, membrane topology of the HCN1 channel, including six transmembrane domains (S1–S6), the cyclic-nucleotide binding site (CNBD), and the GYG K^+ selectivity sequence in the pore domain. Below, a sequence alignment between the S4 region of the HCN1, spHCN, and Shaker K^+ channels (Gauss et al., 1998; Männikkö et al., 2002). The positively charged residues are in bold. The stars above the HCN1 channel note residues mutated into cysteines in this study. The arrows indicate mutations that expressed in oocytes: R247C, T249C, I251C, S253C, L254C, and S261C. (B) HCN1 currents elicited by voltage steps in −10 mV increments from 0 to −190 mV, from a holding potential of 0 mV, followed by a step to +50 mV for tail currents. (C) Representative G(V) curves from isochronal tails at +50 mV for the expressing mutations: (○) R247C: $V_{1/2}$ = −102 ± 1 mV, slope = 12.7 ± 0.9 mV; (●) T249C: $V_{1/2}$ = −118.6 ± 0.8 mV, slope = 13 ± 0.4 mV; (□) S253C: $V_{1/2}$ = −48.8 ± 1.5 mV, slope = 19.5 ± 1.3 mV; (■) L254C: $V_{1/2}$ = −78.8 ± 0.6 mV, slope = 10.7 ± 0.5 mV; (△) S261C: $V_{1/2}$ = −135 ± 6 mV, slope = 22 ± 2 mV; and the background channel (×) C318S: $V_{1/2}$ = −70.2 ± 0.6 mV, slope = 12.3 ± 0.6 mV.

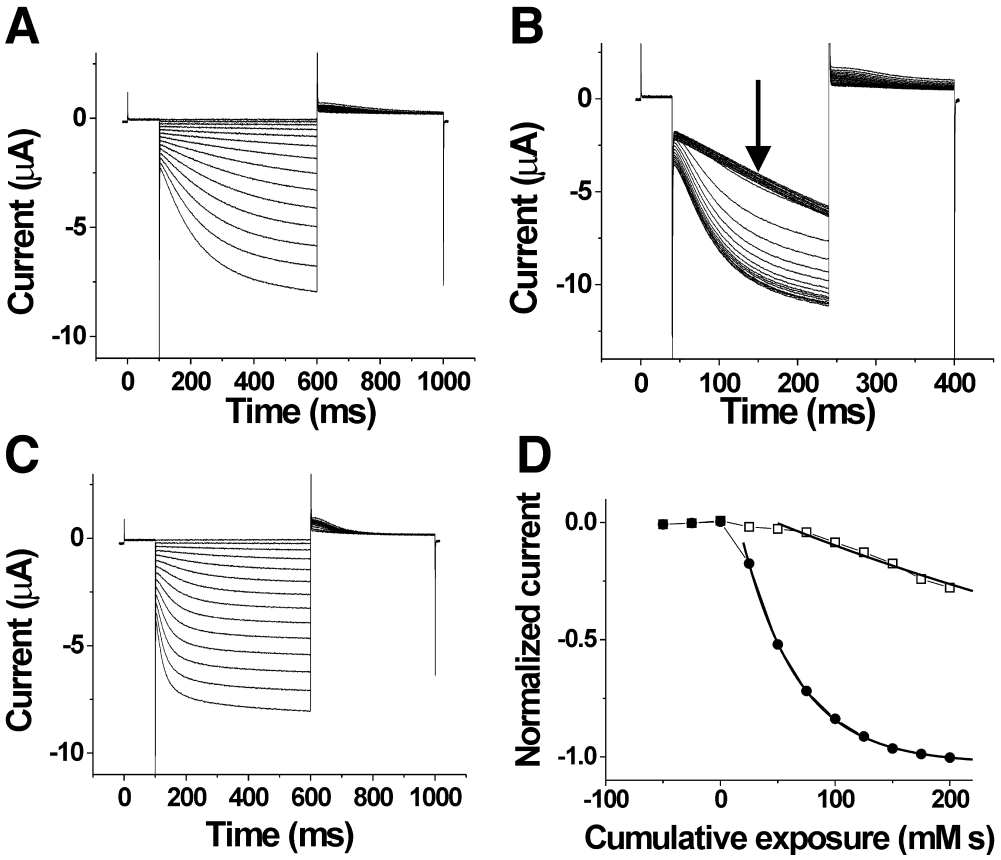

FIGURE 3. State-dependent accessibility of S253C. Currents before (A), during (B), and after (C) the application of 100 μM extracellular MTSET. In A and C, the voltage steps are in −10-mV increments from 0 to −150 mV. In B, voltage was held at 0 mV and then stepped to −120 mV for the test pulse, followed by a step to +50 mV for tail currents. The holding potential was 0 mV. MTSET was applied for 10 s during each episode. (D) Currents measured at the arrow in B as a function of cumulative exposure to MTSET. The modification time course for the extracellular application of 100 μM MTSET at 0 mV (●) and at −100 mV (□). The bold lines are an exponential fit to the data.

S253C almost 10-fold faster at 0 mV than at −100 mV (Fig. 3 D, Table I), suggesting that S253C is more accessible from the extracellular solution at depolarized potentials than at hyperpolarizing potentials. This state dependence is similar to that which was found for S338C in spHCN channels.

We next attempted to test the state dependence of intracellular accessibility for S253C to determine whether it also was similar to the state dependence of S338C in spHCN channels. However, in excised patches, S253C failed to express sufficiently to be tested for intracellular accessibility to MTS reagents. Channels with a cysteine mutant at the neighboring residue L254C, however, expressed at high-enough levels to detect current changes in excised patches. MTSET, in combination with hyperpolarizing steps to activate HCN1 currents, was found to be detrimental to patch stability, prompting the use of MTSEA instead (see MATERIALS AND METHODS). At 0 mV and −120 mV (Fig. 4, A–D), the intracellular application of 100 μM MTSEA onto HCN1 C318S channels (used as our control) caused no significant changes in current amplitudes or current kinetics beyond the normal run-down associated with patch excision (see MATERIALS AND METHODS and Chen et al.,

TABLE I

Modification Rate Constants for Mutants R247C, T249C, I251C, S253C, and L254C

	Extracellular modification		Intracellular modification	
Cysteine mutation	−100 mV	0 mV	−120/−140 mV	0 mV
	$M^{-1}s^{-1}$	$M^{-1}s^{-1}$	$M^{-1}s^{-1}$	$M^{-1}s^{-1}$
R247C	350 ± 60 (n = 3)	650 ± 280 (n = 3)	Poor expression	
T249C	2.9 ± 1.0 (n = 4)	13.5 ± 4.5 (n = 3)	Poor expression	
I251C	No effect (n = 9)		Poor expression	
S253C	1.2 ± 0.24 (n = 3)	9.2 ± 1.6 (n = 5)	Poor expression	
L254C	No effect (n = 3)		1,540 ± 420 (n = 6)	<10 (n = 6)
S261C	Not tested		151 ± 9 (n = 3)	<10 (n = 5)

Values given as mean ± SEM (n). k is the second-order rate constant for MTS modification of the specified channels at the indicated potentials. "No effect" means that 1 mM MTSET for 2 min affected the current by <10%; thus, k < 1 $M^{-1}s^{-1}$.

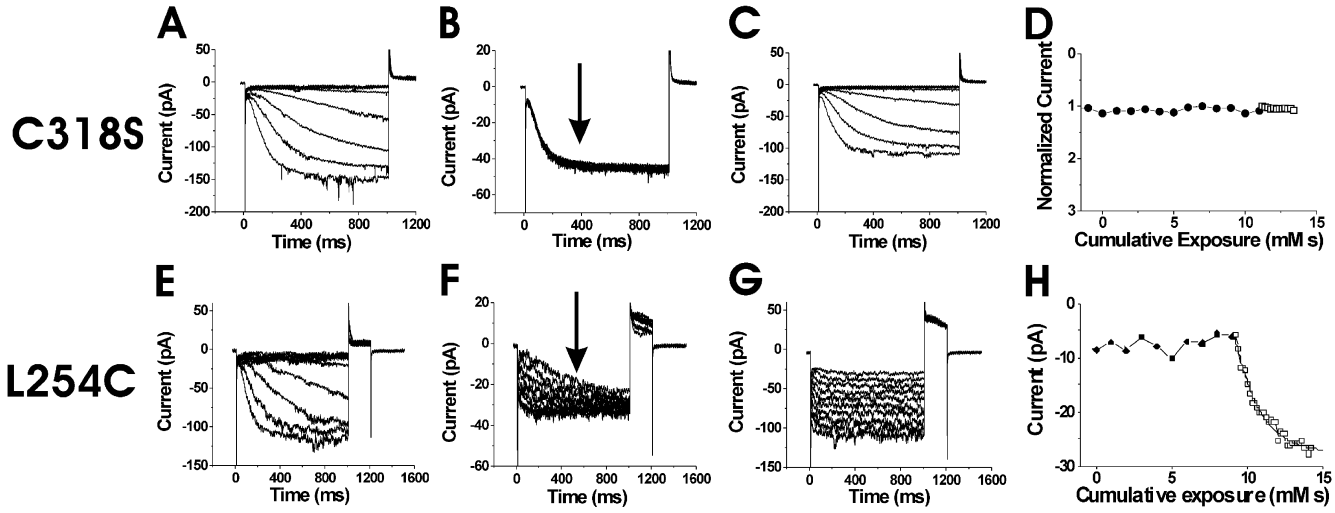

FIGURE 4. State-dependent accessibility of L254C. (A–D) Application of MTSEA on the background channel HCN1 C318S. Currents before (A), during (B), and after (C), the intracellular application of MTSEA onto inside-out patches expressing HCN1 C318S mutants. In A and C the voltage steps occur in −10-mV increments from 0 to −120 mV. In B, the current trace is from a voltage step from 0 to −120 mV for 1 s during the application of 100 μM MTSEA. The voltage steps occurred every 2 s. (D) Currents measured at the arrow in B as a function of cumulative exposure to MTSEA. Modification rates for MTSEA at 0 mV (●) and at −120 mV (○). (E–H) State-dependent accessibility of L254C. Currents before (E), during (F), and after (G) the application of 100 μM intracellular MTSEA. In E and G, the voltage steps occur in 10-mV increments from −40 to −150 mV. In F, voltage was held at 0 mV and then stepped to −120 mV for the test pulse, followed by a step to +50 mV for tail currents. The holding potential was −120 mV. The patch was excised into a bath solution containing 100 μM MTSEA. (H) Currents measured at the arrow in F as a function of cumulative exposure to MTSEA. Modification time course for intracellular MTSEA at 0 mV (●) and −120 mV (□). The current amplitudes are plotted versus cumulative exposure to MTSEA and MTSET, in D and H, respectively. The bold line is an exponential fit to the data in H.

2001). In contrast to this control recording, the intracellular application of MTSEA eliminated the voltage dependence of L254C currents (Fig. 4, E–G), similar to the effects from the intracellular application of MTSET in the spHCN channel residues S338C and L340C (Männikkö et al., 2002). The intracellular application of MTSEA modified L254C much faster at −120 mV than at 0 mV (Fig. 4 H, Table I), which is the opposite result to the voltage dependence seen from the extracellular application of MTSET on S253C. This finding suggests that L254C is more accessible from the intracellular side of the membrane at hyperpolarizing potentials than at depolarizing potentials. The extracellular application of MTSET and MTSEA had no effect on L254C, suggesting that L254C was never exposed to the extracellular solution. These findings of extracellular accessibility from S253C and extracellular/intracellular accessibility from L254C point to a transmembrane movement of the middle portion of S4 at residues 253 and 254.

We next tested the accessibility of residues in proximity to 253 and 254 for the state dependence of MTSET modification. We attempted to test the accessibility of residue R259C; however, this mutation did not express. Subsequent mutations on the adjacent residues L258C and L260C failed to express as well. S261C did express, and so this residue was used to test for internal accessibility (Fig. 5, A–D). We found that the intracellular application of 200 μM MTSEA modified S261C faster at −140 mV than at 0 mV (Fig. 5 D, Table I). This result suggests that S261C is more accessible from the intracellular side at hyperpolarizing potentials than at depolarizing potentials.

The mutant K250C, the next charged residue in the direction of the NH_2-terminal, did not express, so we used I251C—an adjacent, uncharged residue. The extracellular application of MTSET to I251C did not affect currents either at 0 or −100 mV (Table I). Intracellular accessibility studies were attempted on I251C, to test the range in intracellular S4 movement, but poor expression in patches prevented analysis. Thus, it remains unknown whether accessibility of I251C is state-dependent.

The extracellular application of MTSET onto R247C mutants dramatically decreased the deactivation times of tail currents (Fig. 5, E–G). There was only a small difference in the MTSET modification rates between hyperpolarizing and depolarizing potentials (Fig. 5 H, Table I), indicating that R247C is exposed to the extracellular solution both at depolarizing and hyperpolarizing potentials. The results for R247C are similar to the results for R332C, the homologous residue in spHCN channels (Männikkö et al., 2002).

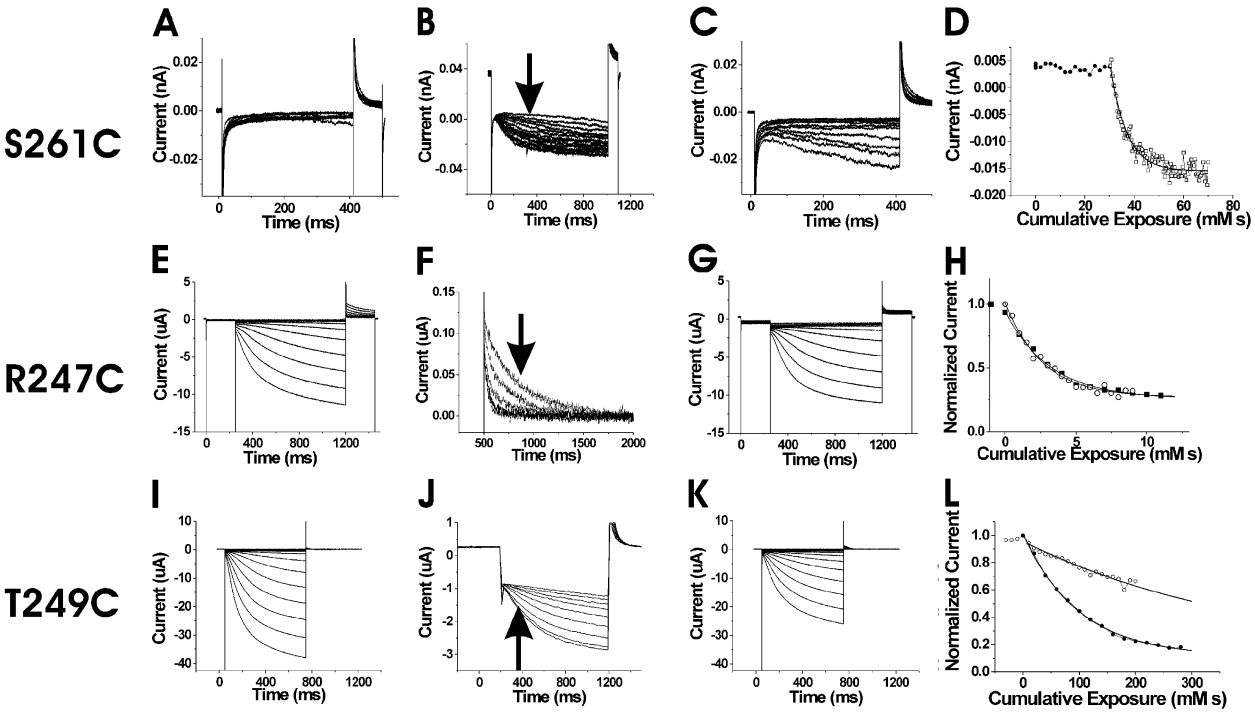

FIGURE 5. State-dependent accessibility of three S4 residues. (A–D) State-dependent accessibility of S261C. Currents before (A), during (B), and after (C) the intracellular application of 200 μM MTSEA. In (A) and (C), the voltage steps occur in –10 mV increments from −60 to −150 mV. In B, the voltage was held at 0 mV and then stepped to −140 mV for the test pulse, followed by a step to +50 mV for tail currents. The holding potential was 0 mV. The patch was excised into a bath containing 200 μM MTSEA. (D) Modification time course for intracellular MTSEA at 0 mV (●) and −140 mV (□). The current amplitudes are plotted versus their cumulative exposure to MTSEA. The bold line is an exponential fit. (E–G) State-independent accessibility of R247C. Currents before (E), during (F), and after (G) the extracellular application of 100 μM MTSET. In E and G, the voltage steps occur in −10-mV increments from 0 to −150 mV. In F, voltage was held at 0 mV and then stepped to −120 mV for the test pulse, followed by a step to 0 mV for tail currents. The tail currents during the application of 100 μM MTSET are shown in F. (H) Currents at the arrow in F as a function of cumulative exposure to MTSET. The modification time course for the extracellular application of MTSET at 0 mV (●) and at −100 mV (□). The bold lines are exponential fits to the data. (I–L) State-dependent accessibility of T249C. Currents before (I), during (J), and after (K) the application of 2 mM extracellular MTSET. In I and K, the voltage steps occur in −10-mV increments from 0 to −150 mV. In J, voltage was held at 0 mV and then stepped to −120 mV for the test pulse, followed by a step to +50 mV for tail currents. The holding potential was 0 mV. MTSET was applied for 10 s during each episode. (L) Currents at the arrow in J as a function of cumulative exposure to MTSET. Modification time course for the extracellular application of MTSET at 0 mV (●) and at −100 mV (□).

The extracellular application of MTSET onto T249C mutants resulted in a shift in voltage activation to more hyperpolarizing potentials by ∼10 mV. This modification was state dependent, with modification rates faster at 0 mV than −100 mV (Fig. 5, I–L, Table I; see also DISCUSSION). The voltage-dependent modification rates suggest that T249C moves from an extracellularly accessible location at depolarizing potentials to an inaccessible position at hyperpolarizing potentials. R247C and T249C did not express well enough to test for intracellular accessibility.

The state-dependent pattern of cysteine accessibility is very similar between spHCN (Männikkö et al., 2002) and HCN1 channels (this study), suggesting that S4 has a similar role in these two channels and that S4 is the voltage sensor in both these channels. However, the gating behavior of spHCN channels is quite different from the gating behavior in HCN1 channels: HCN1 channels do not inactivate, while spHCN channels display an inactivation that can be removed by a high concentration of cAMP (Fig. 6, A and B). spHCN channels also activate at more depolarized potentials than mammalian HCN channels (Gauss et al., 1998; Ludwig et al., 1998).

The cAMP-binding site is in the COOH terminus that contains a consensus cyclic nucleotide binding domain (CNBD). Earlier studies have shown that deleting the COOH terminus (including the CNBD) from mammalian HCN channels eliminates the cAMP-induced voltage shifts (Wainger et al., 2001). To elucidate the role of the COOH terminus in the different gating behavior between spHCN channels and HCN1 channels, we constructed a COOH-terminal–deleted spHCN channel $spHCN_{\Delta C\text{-term}}$ (see MATERIALS AND METHODS). spH-

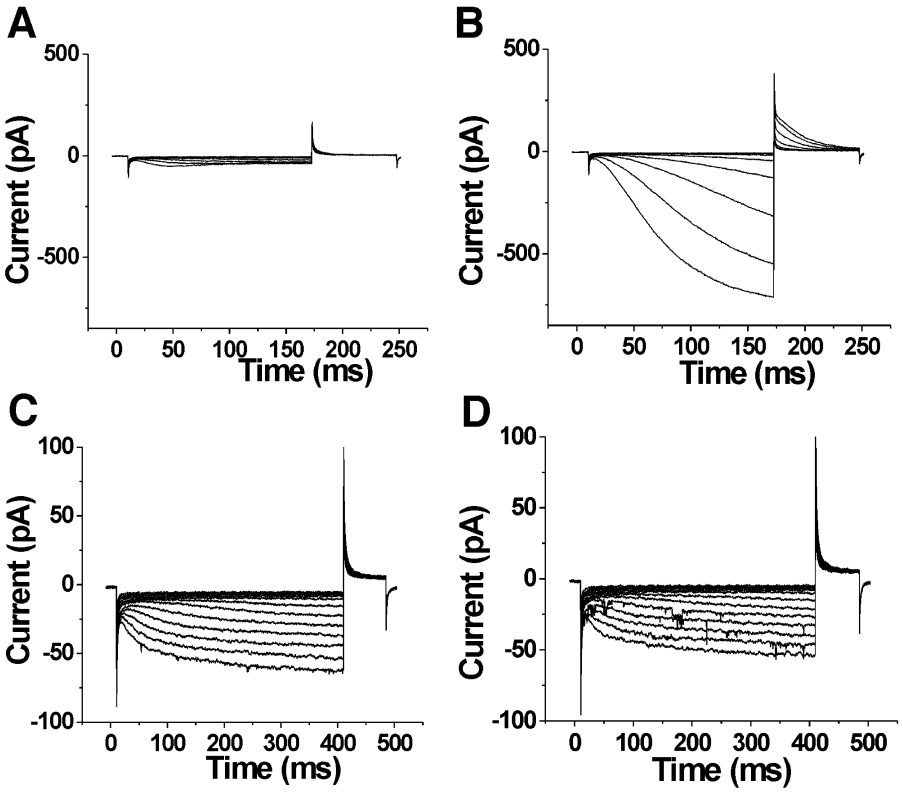

FIGURE 6. The COOH terminus is necessary for inactivation in spHCN channels. Currents in the absence of internal cAMP (A and C) or the presence of 100 μM cAMP (B and D) in inside-out patches expressing wt spHCN channels (A and B) and $spHCN_{\Delta C\text{-term}}$ channels (C and D). For the wt spHCN channels, voltage steps occurred in 10-mV increments from −10 to −120 mV, from a holding potential of −10 mV. Tails currents were at +50 mV. For the $spHCN_{\Delta C\text{-term}}$ channels, voltage steps occurred in 10-mV increments from −10 to −160 mV, from a holding potential of −10 mV. Tail currents were at +50 mV. The effects of the truncation of the COOH terminus of spHCN channels are: (1) the removal of inactivation, (2) a shift in the voltage dependence by −25 mV (see text), and (3) a 10-fold reduction in the expression level. (Note that spHCN channels in the excised patches activated at 20–30-mV more negative potentials than in intact oocytes, Männikkö et al., 2002.).

$CN_{\Delta C\text{-term}}$ channels did not inactivate in 0 cAMP solutions, in contrast to wt spHCN channels (n = 3, Fig. 6 C). In addition, the amplitude of the current through $spHCN_{\Delta C\text{-term}}$ channels did not change with cAMP concentration, in contrast to wt spHCN channels (n = 3, Fig. 6 D). The absence of inactivation in $spHCN_{\Delta C\text{-term}}$ channels shows that the inactivation of spHCN channels is not an intrinsic property of the transmembrane-containing portion (S1–S6) of spHCN channels, but requires the presence of the COOH terminus. In addition, the $spHCN_{\Delta C\text{-term}}$ channels activated at more hyperpolarized potentials ($V_{1/2}$ = −73 ± 6 mV and z = 3.3 ± 0.9, n = 3) than the wt spHCN channels ($V_{1/2}$ = −47 ± 3 mV and z = 3.2 ± 0.5, n = 3). The COOH terminus–truncated versions of spHCN and HCN1 channels activated in a similar voltage range (Fig. 2 C), suggesting that the COOH terminus of spHCN channels is, at least partly, responsible for the more depolarized voltage range of activation of spHCN channels.

DISCUSSION

Using cysteine accessibility methods, we found that S4 moves in a voltage-dependent manner in HCN1 channels (Table I and Fig. 7 C). The opposite state-dependent accessibility of two neighboring residues, S253C and L254C, suggests that the middle portion of S4 moves completely across the membrane when the HCN1 channel goes from the closed state to the open state (Fig. 7, A and B). This S4 movement is similar to the S4 movement previously found in spHCN channels (Männikkö et al., 2002) and in Shaker K^+ channels (Larsson et al., 1996; Baker et al., 1998), in which residues S338 in spHCN and R368 in Shaker K^+ channels (homologous to S253 in the HCN1 channel) exhibited a voltage-dependent transmembrane movement from the intracellular solution to the extracellular solution. Data from other cysteine mutations, such as S261C and T249C, provide additional support for a similar S4 motion in spHCN and HCN1 channels, and for a similar voltage-sensing mechanism in these channels (Fig. 7, A and B). However, Bell et al. (2004, in this issue) tested more intracellular residues and found that the intracellular S4 region that displayed state-dependent modification was significant larger than the state-dependent extracellular S4 region. Therefore, we also suggest an alternative model for S4 movement in HCN channels (Fig. 7, D and E), in which the S4 helix unwinds in the middle when S4 moves inward. This model is compatible with our data and provides an explanation for the smaller region of state-dependent modification at the external membrane border of S4 (Table I; and see Bell et al., 2004, in this issue).

In general, the state dependence of intracellular modification was larger than that of extracellular modification (Fig. 7 C). This finding could be due to the limited voltage range for testing MTSET accessibility in intact oocytes (−100 to +50 mV), in combination with the fact that most of the cysteine-introduced HCN1

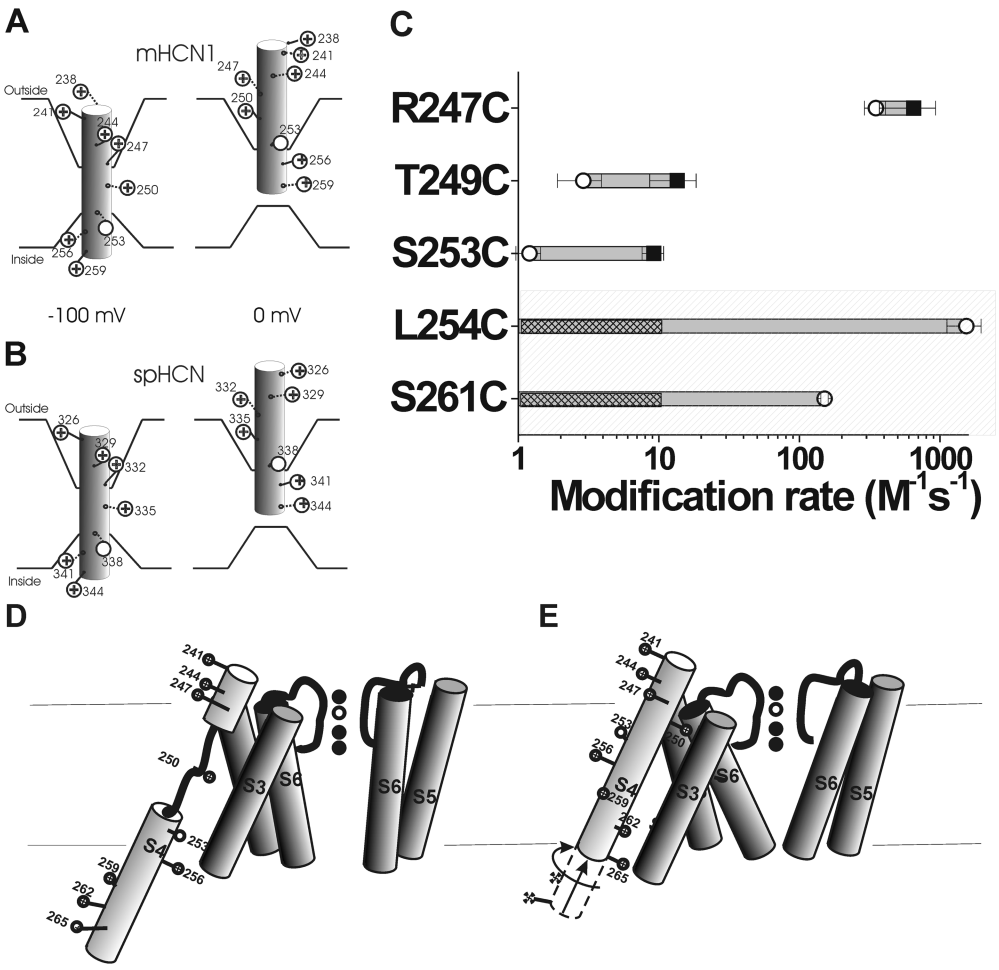

FIGURE 7. A model of the voltage-dependent movements of S4 in the HCN1 channel (A) and the spHCN channel (B). (A) Based on results from this study, S4 is the voltage sensor in the HCN1 channel. HCN1 S4 is in an inward position at −100 mV, which opens the channel gate. Stepping the voltage to 0 mV results in the outward movement of S4 into the extracellular solution, causing the channel gate to close. This movement is similar to that described for the spHCN channel (Männikkö et al., 2002), seen in B. The intracellular border of S4 movement is not well-defined from our results. (C) Modification rates for cysteine mutants in the HCN1 channel in the open (○) and closed (■) states. The shaded area represents residues tested for intracellular accessibility by excised patch recordings. The nonshaded area represents residues tested for extracellular accessibility by two-electrode voltage clamp. We did not see any modification resulting from the intracellular application of MTSEA at 0 mV; hence, we can only give an upper estimate of the modification rate for these residues. The hatch bars indicate the range of possible modification rates for these residues at 0 mV. (D and E) An alternative model for S4 movement in HCN1 channels. At hyperpolarized potentials (D), the S4 α helix unwinds external to the S253 as it moves inwards. At depolarized potentials (E), the lower portion of S4 moves outwards and S4 undergoes a conformational change into a continuous α helix.

channels activated in a very hyperpolarized voltage range (-135 mV $< V_{1/2} < -50$ mV; Fig. 2 C). We tested intracellular modification for closed channels at 0 mV, which is >50 mV from the mid-point of the activation curve. In most batches of oocytes, we were unable to test extracellular modification for open channels held at more negative potentials than −100 mV, a potential at which a significant number of channels remain closed, and, hence, a substantial number of S4s are most likely not in their activated position (Fig. 7 A). The possibility that a substantial number of S4s are still in their resting position at −100 mV, could lead to an underestimation of the change in modification rate between closed and open channels. At a particular voltage, one could estimate the number of S4s in their resting position and activated position from the G(V), but this estimation is very model dependent. For example, S4 in HCN channels could move in several steps, and some of these steps could be concerted conformational changes in all four subunits, as has been suggested for Shaker K channels (Baker et al., 1998; Schoppa and Sigworth, 1998; Mannuzzu and Isacoff, 2000; Loboda and Armstrong, 2001). If this were the case, then for a cysteine residue that becomes buried in a final concerted step, a fraction f of channels that are still closed would result in a fraction f of those cysteines to be accessible. On the other hand, a simple Hodgkin and Huxley model (four independent S4s with only one resting position and one activated position) would, at the same open probability, predict that a much smaller fraction of these cysteines would be accessible (see Bell et al., 2004, in this issue). A gating charge versus voltage curve would give a better estimate of how many S4s are in the resting position relative to the activated position at any potential. To this day, there are no published recordings of gating currents from HCN1 channels. However, we were able to measure the external accessibility of 249C at −130 mV in one batch of oocytes

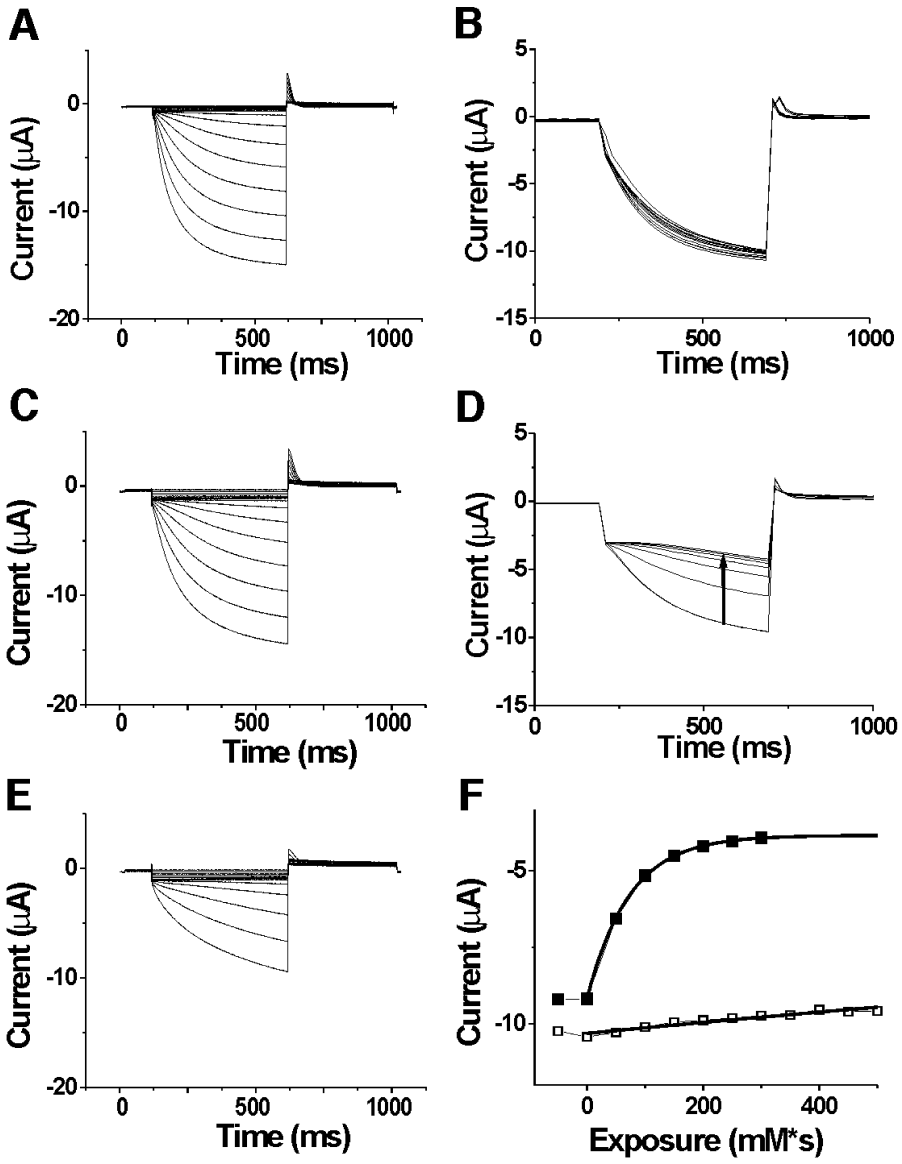

FIGURE 8. Larger state-dependent modification of T249C at more hyperpolarized potentials. Currents before (A), during (B), and after (C) the application of 10 mM extracellular MTSET applied at −130 mV. Currents during (D) and after (E) the application of 10 mM extracellular MTSET applied at 0 mV on the same oocyte as in A to C. In A, C, and E, the voltage steps are in −10-mV increments from 0 to −140 mV. In B and D, the voltage was held at 0 mV and then stepped to −120 mV for the test pulse, followed by a step to +50 mV for tail currents. The holding potential was 0 mV. MTSET was applied for 5 s between each episode. (F) Currents measured at the arrow in D as a function of cumulative exposure to MTSET. The modification time course for extracellular application of MTSET at 0 mV (■) and at −130 mV (□). The bold lines are an exponential fit to the data (for −130 mV, the I_4 was constrained to the value found for the fit at 0 mV). τ = 3.5 M*s for −130 mV, and τ = 0.0727 M*s for 0 mV. Similar results were seen in four oocytes.

(Fig. 8). The modification rate at −130 mV was >40-fold slower at −130 mV than at 0 mV, measured in the same oocyte ($k < 0.33\ M^{-1}s^{-1}$ at −130 mV; $k = 13.5\ M^{-1}s^{-1}$ at 0 mV, $n = 4$). From the limiting data on extracellular accessibility at extremely negative voltages, we have concluded that the accessibility of S4 changes with voltage both at the extracellular and the intracellular membrane border. Hence, we conclude that S4 movement is similar in HCN1 channels and spHCN channels.

However, there are significant functional differences between spHCN channels and mammalian HCN1 channels, in particular the presence of a cAMP-dependent inactivation in spHCN (Gauss et al., 1998), which is absent in mammalian HCN channels. In addition, spHCN channels open in a more depolarized voltage range (Gauss et al., 1998; Ludwig et al., 1998). We found that the deletion of the COOH terminus in spHCN channels removed the inactivation of spHCN channels, showing that the inactivation of spHCN channels is not an intrinsic property of the transmembrane-containing portion (S1–S6) of spHCN. This inactivation can also be removed by high concentrations of cAMP that presumably bind to the CNBD domain in the COOH terminus. The removal of inactivation by either high concentrations of cAMP or by a COOH-terminal deletion mutation lead us to suggest a model for the inactivation of spHCN channels that is similar to a model proposed to explain the cAMP-dependent voltage shifts in the mammalian HCN channels (Wainger et al., 2001). In the model proposed by Wainger et al. (2001), in the absence of cAMP the COOH terminus inhibits the transmembrane-containing portion of the HCN channel, causing a hyperpolarizing shift in the

voltage dependence. The binding of cAMP to the COOH terminus or the deletion of the COOH terminus relieves this inhibition, resulting in the shift of the voltage dependence to more depolarized potentials (Wainger et al., 2001). We propose that in spHCN channels, at low cAMP the COOH terminus interacts with the transmembrane-containing portion (S1–S6) of spHCN, causing the inactivation of spHCN channels and a reduction in current amplitude. High concentrations of cAMP or a deletion of the COOH terminus removes this interaction, thus relieving the inactivation.

The deletion of the COOH terminus also shifted the voltage dependence of spHCN channels by −25 mV, making the truncated spHCN channels open in a voltage range similar to the voltage range in the mammalian HCN channels. In contrast, the truncation of HCN1 channels shifted the activation range of HCN1 channels only by a very small amount in the opposite direction (+5 mV; Wainger et al., 2001), suggesting that the more depolarized activation range of spHCN channels could be due to the stabilization of the open state relative the closed state by the COOH terminus. This effect is opposite to the one seen in mammalian HCN channels, where the COOH terminus stabilizes the closed state (Wainger et al., 2001). In addition, this effect in spHCN channels is not modulated by cAMP, whereas the effect in mammalian HCN channels is cAMP dependent (Wainger et al., 2001). One attractive mechanism for the effect seen in spHCN channels is an electrostatic interaction between some of the positive charges in S4 and some negative charges in the COOH terminus of spHCN channels. This interaction would stabilize the inward position of S4 and, hence, would shift the voltage dependence to more depolarized potentials. The COOH terminus in spHCN channels contains additional negative charges that are not present in the mammalian HCN channels. In the crystal structure of the COOH-terminal domain of HCN2 channels (Zagotta et al., 2003), several of these additional negative charges are located on the surface of this structure, where they could possibly interact with other domains of the channel (e.g., with positive charges in S4). Another possibility is that the COOH terminus in spHCN channels destabilizes the closed state by directly affecting S6, which has been suggested to be the activation gate of HCN channels (Shin et al., 2001; Rothberg et al., 2002). This hypothesis is supported by the activation kinetics slowing in the COOH terminus–deleted spHCN channels at extreme negative potentials (Fig. 6). Further studies are necessary to elucidate the mechanism of COOH terminus modulation of spHCN channels and to determine whether the difference between spHCN and mammalian HCN channels is caused by a difference in the COOH terminus or a difference in the interaction between the COOH terminus and the core domain. However, it is clear that the COOH terminus of spHCN channels has two effects on spHCN channels: a cAMP-dependent effect that causes inactivation and a cAMP-independent effect that shifts the voltage dependence into a more depolarized voltage range.

Our cysteine accessibility results suggest that the four most NH_2-terminal S4 charges in HCN1 channels (K238, R241, R244, and R247) and the three most NH_2-terminal S4 charges in spHCN channels (R326, K329, and R332) (Männikkö et al., 2002) are not part of the voltage sensor. The state-independent accessibility of R247 in HCN1 channels, and R326C and R332C in spHCN channels (Männikkö et al., 2002) indicate that these charges are always exposed to the extracellular solution and, hence, do not significantly contribute to the voltage sensor since they do not traverse a significant part of the electric field. However, the neutralization of these charges changes the voltage dependence by shifting the activation curve to more negative potentials in both spHCN channels and mammalian HCN channels (Chen et al., 2000;Vaca et al., 2000; Männikkö et al., 2002). Chen et al. (2000) showed that altering the charge on the corresponding residues in HCN2 channels alters the size of Mg^{2+}-induced voltage shifts in a manner consistent with these residues functioning as surface charges. Our results, showing that these residues are always exposed to the extracellular solution, support the hypothesis by Chen et al. (2000) that these charges function as surface charges. Alternatively, these most external charges might serve to stabilize the closed state or destabilize the open state by interacting with other charged parts of the channel. The neutralization of these charges could, therefore, shift the equilibrium between the open and closed states, giving rise to the observed voltage shifts. In both cases, these external residues only indirectly influence the voltage sensitivity of HCN channels since they do not directly form part of the voltage sensor of HCN channels.

These external charges are conserved among HCN channels. Why are these charges conserved if they are not part of the voltage sensor? Our results are consistent with the hypothesis that these charges function as surface charges. We hypothesize that these surface charges are necessary for the HCN channels to open in a physiologically relevant voltage range. This hypothesis is based on the finding that the removal of these charges in mammalian HCN channels shifts the voltage dependence to such negative potentials that, under normal physiological conditions ($V > -80$ mV), these channels seldom open (Chen et al., 2000; Vaca et al., 2000).

Hyperpolarization-activated HCN channels appear to share a similar S4 movement with depolarization-activated Kv channels. However, in HCN channels, the out-

ward movement of S4 is related to channel closing, and the inward movement of S4, to channel opening. These S4 movements are the opposite from those in Shaker K^+ channels, where the outward movement of S4 leads to channel opening and the inward movement leads to channel closing. The coupling mechanism between the movement of the voltage sensor and the opening of the activation gate remains undefined for both HCN channels and Kv channels (Larsson, 2002). A more detailed analysis of the movement of S4 and the identification of the molecular interactions between S4 and the pore region S5-S6 in HCN and Kv channels may give more insight into the coupling mechanisms of these two classes of channels and could help explain the structural basis for the opposite voltage dependence of activation that exists between hyperpolarization- and depolarization-activated channels.

We thank Drs. Fredrik Elinder and Hans Koch for comments and suggestions; and Sandra Oster for editing the manuscript.

This study was supported by a grant from National Institutes of Health (NS043259) to H.P. Larsson.

Olaf S. Andersen served as editor.

Submitted: 7 August 2003
Accepted: 31 October 2003

REFERENCES

Aggarwal, S.K., and R. MacKinnon. 1996. Contribution of the S4 segment to gating charge in the Shaker K^+ channel. *Neuron.* 16: 1169–1177.

Baker, O.S., H.P. Larsson, L.M. Mannuzzu, and E.Y. Isacoff. 1998. Three transmembrane conformations and sequence-dependent displacement of the S4 domain in shaker K^+ channel gating. *Neuron.* 20:1283–1294.

Bell, D.C., H. Yao, R.C. Saenger, J.H. Riley, and S.A. Siegelbaum. 2004. Changes in local S4 environment provide a voltage-sensing mechanism for mammalian hyperpolarization-activated HCN channels. *J. Gen. Physiol.* 123:5–19.

Chen, J., J.S. Mitcheson, M. Lin, and M.C. Sanguinetti. 2000. Functional roles of charged residues in the putative voltage sensor of the HCN2 pacemaker channel. *J. Biol. Chem.* 275:36465–36471.

Chen, S., J. Wang, and S.A. Siegelbaum. 2001. Properties of hyperpolarization-activated pacemaker current defined by coassembly of HCN1 and HCN2 subunits and basal modulation by cyclic nucleotide. *J. Gen. Physiol.* 117:491–504.

Gauss, R., R. Seifert, and U.B. Kaupp. 1998. Molecular identification of a hyperpolarization-activated channel in sea urchin sperm. *Nature.* 393:583–587.

Holmgren, M., Y. Liu, Y. Xu, and G. Yellen. 1996. On the use of thiol-modifying agents to determine channel topology. *Neuropharmacology.* 35:797–804.

Karlin, A., and M.H. Akabas. 1998. Substituted-cysteine accessibility method. *Methods Enzymol.* 293:123–145.

Larsson, H.P., O.S. Baker, D.S. Dhillon, and E.Y. Isacoff. 1996. Transmembrane movement of the Shaker K^+ channel S4. *Neuron.* 16:387–397.

Larsson, H.P. 2002. The search is on for the voltage sensor-to-gate coupling. *J. Gen. Physiol.* 120:475–481.

Loboda, A., and C.M. Armstrong. 2001. Resolving the gating charge movement associated with late transitions in K channel activation. *Biophys. J.* 81:905–916.

Ludwig, A., X. Zong, M. Jeglitsch, F. Hofmann, and M. Biel. 1998. A family of hyperpolarization-activated mammalian cation channels. *Nature.* 393:587–591.

Männikkö, R., F. Elinder, and H.P. Larsson. 2002. Voltage-sensing mechanism is conserved among ion channels gated by opposite voltages. *Nature.* 419:837–841.

Mannuzzu, L.M., and E.Y. Isacoff. 2000. Independence and cooperativity in rearrangements of a potassium channel voltage sensor revealed by single subunit fluorescence. *J. Gen. Physiol.* 115:257–268.

Robinson, R.B., and S.A. Siegelbaum. 2003. Hyperpolarization-activated cation currents: from molecules to physiological function. *Annu. Rev. Physiol.* 65:453–480.

Rothberg, B.S., K.S. Shin, P.S. Phale, and G. Yellen. 2002. Voltage-controlled gating at the intracellular entrance to a hyperpolarization-activated cation channel. *J. Gen. Physiol.* 119:83–91.

Santoro, B., D.T. Liu, H. Yao, D. Bartsch, E.R. Kandel, S.A. Siegelbaum, and G.R. Tibbs. 1998. Identification of a gene encoding a hyperpolarization-activated pacemaker channel of brain. *Cell.* 93: 717–729.

Santoro, B., and G.R. Tibbs. 1999. The HCN gene family: molecular basis of the hyperpolarization-activated pacemaker channels. *Ann. NY Acad. Sci.* 868:741–764.

Schoppa, N.E., and F.J. Sigworth. 1998. Activation of Shaker potassium channels. III. An activation gating model for wild-type and V2 mutant channels. *J. Gen. Physiol.* 111:313–342.

Seoh, S.A., D. Sigg, D.M. Papazian, and F. Bezanilla. 1996. Voltage-sensing residues in the S2 and S4 segments of the Shaker K^+ channel. *Neuron.* 16:1159–1167.

Sesti, F., S. Rajan, R. Gonzalez-Colaso, N. Nikolaeva, and S.A. Goldstein. 2003. Hyperpolarization moves S4 sensors inward to open MVP, a methanococcal voltage-gated potassium channel. *Nat. Neurosci.* 6:353–361.

Shin, K.S., B.S. Rothberg, and G. Yellen. 2001. Blocker state dependence and trapping in hyperpolarization-activated cation channels: evidence for an intracellular activation gate. *J. Gen. Physiol.* 117:91–101.

Stauffer, D.A., and A. Karlin. 1994. Electrostatic potential of the acetylcholine binding sites in the nicotinic receptor probed by reactions of binding-site cysteines with charged methanethiosulfonates. *Biochemistry.* 33:6840–6849.

Vaca, L., J. Stieber, X. Zong, A. Ludwig, F. Hofmann, and M. Biel. 2000. Mutations in the S4 domain of a pacemaker channel alter its voltage dependence. *FEBS Lett.* 479:35–40.

Wainger, B.J., M. DeGennaro, B. Santoro, S.A. Siegelbaum, and G.R. Tibbs. 2001. Molecular mechanism of cAMP modulation of HCN pacemaker channels. *Nature.* 411:805–810.

Xue, T., and R.A. Li. 2002. An external determinant in the S5-P linker of the pacemaker (HCN) channel identified by sulfhydryl modification. *J. Biol. Chem.* 277:46233–46242.

Yusaf, S.P., D. Wray, and A. Sivaprasadarao. 1996. Measurement of the movement of the S4 segment during the activation of a voltage-gated potassium channel. *Pflugers Arch.* 433:91–97.

Zagotta, W.N., N.B. Olivier, K.D. Black, E.C. Young, R. Olson, and E. Gouaux. 2003. Structural basis for modulation and agonist specificity of HCN pacemaker channels. *Nature.* 425:200–205.